



Article

Germline Mutation Enrichment in Pathways Controlling Endothelial Cell Homeostasis in Patients with Brain Arteriovenous Malformation: Implication for Molecular Diagnosis

Concetta Scimone ^{1,2}, Francesca Granata ³, Marcello Longo ³, Enricomaria Mormina ^{3,4}, Cristina Turiaco ³, Antonio A. Caragliano ³, Luigi Donato ^{1,2,*}, Antonina Sidoti ^{1,2,*} and Rosalia D'Angelo ^{1,2}

¹ Department of Biomedical, Dental, Morphological and Functional Imaging Sciences, University of Messina, Via Consolare Valeria 1, 98125 Messina, Italy; cscimone@unime.it (C.S.); rdangelo@unime.it (R.D.)

² Department of Biomolecular Strategies, Genetics and Avant-Garde Therapies, I.E.ME.S.T., Via Michele Miraglia, 90139 Palermo, Italy

³ Neuroradiology Unit—Department of Biomedical, Dental, Morphological and Functional Imaging Sciences, University of Messina, Via Consolare Valeria 1, 98125 Messina, Italy; fgranata@unime.it (F.G.); mlongo@unime.it (M.L.); enricomaria.mormina@gmail.com (E.M.); cettinascimone.cs@gmail.com (C.T.); caraglia1987@gmail.com (A.A.C.)

⁴ Department of Clinical and Experimental Medicine, University of Messina, Consolare Valeria 1, 98125 Messina, Italy

* Correspondence: ldonato@unime.it (L.D.); asidoti@unime.it (A.S.); Tel.: +39-0902213378 (L.D.); +39-0902213370 (A.S.)

Received: 7 May 2020; Accepted: 15 June 2020; Published: 17 June 2020



Abstract: Brain arteriovenous malformation (bAVM) is a congenital defect affecting brain microvasculature, characterized by a direct shunt from arterioles to venules. Germline mutations in several genes related to transforming growth factor beta (TGF- β)/BMP signaling are linked to both sporadic and hereditary phenotypes. However, the low incidence of inherited cases makes the genetic bases of the disease unclear. To increase this knowledge, we performed a whole exome sequencing on five patients, on DNA purified by peripheral blood. Variants were filtered based on frequency and functional class. Those selected were validated by Sanger sequencing. Genes carrying selected variants were prioritized to relate these genes with those already known to be linked to bAVM development. Most of the prioritized genes showed a correlation with the TGF- β Notch signaling and vessel morphogenesis. However, two novel pathways related to cilia morphogenesis and ion homeostasis were enriched in mutated genes. These results suggest novel insights on sporadic bAVM onset and confirm its genetic heterogeneity. The high frequency of germline variants in genes related to TGF- β signaling allows us to hypothesize bAVM as a complex trait resulting from the co-existence of low-penetrance loci. Deeper knowledge on bAVM genetics can improve personalized diagnosis and can be helpful with genotype–phenotype correlations.

Keywords: brain arteriovenous malformations; exome sequencing; endothelial properties; molecular diagnosis

1. Introduction

Brain arteriovenous malformations (bAVM, OMIM #108010) are vascular malformations affecting brain vasculature. Lack of a capillary bed and a direct shunt from arterioles to venules, as well as pericyte reduction, are characteristics of the lesions [1]. A vessel tangle is formed, usually called

nidus. During transition from the feeding arteries to the nidus and then, to the draining veins, vessels show dysregulated differentiation patterns and severe enlargement. From arteries, blood perfuses to the nidus with high pressure, increasing risk of lesion rupture. Moreover, the mix of arterial and venous circulations within these lesions leads to a deficit in cerebral tissue oxygenation. This complex condition usually results in major clinical manifestations such as intracerebral hemorrhage and epileptic seizures, appearing in almost 50% of patients. Disease incidence is about 0.01% worldwide and usually arises at an early age [2]. Nevertheless, it most often occurs as a sporadic condition and only a few dozen cases are reported as inherited with an autosomal dominant pattern. Hereditary bAVM usually coexists with other vascular syndromes, such as Osler-Weber-Rendu syndrome, also known as hereditary hemorrhagic telangiectasia (HHT). HHT includes different phenotypes caused by mutations in genes related to the transforming growth factor beta 2 (TGF- β II) transduction pathway, such as *ENG*, *ACVRL1*, *SMAD4*, and *GDF2* [3–5]. Due to the severe remodeling rate and recidivism risk after total surgical resection, bAVMs are considered highly dynamic lesions. Therefore, lesion growth is now thought of as the result of continuous endogenous stimuli due to genetic factors. The low frequency of inherited bAVM makes molecular characterization of the disease difficult. Impaired expression of the ephrin family genes and of other vascular differentiation markers was reported by several authors [6,7]. At the same time, the sporadic nature of the disease can also be considered a result of numerous single nucleotide polymorphisms (SNPs) in genes involved in vasculogenesis and early angiogenesis pathways, as, for instance, in vascular endothelial growth factor (VEGF) and Notch signaling [8]. To improve knowledge on bAVM pathogenesis, we purified DNA from peripheral blood and performed a whole exome sequencing (WES) analysis on a group of five patients affected by sporadic bAVM. Then, we clustered genes carrying the detected mutations, highlighting pathways and prioritizing genes mainly linked to bAVM development.

2. Results

2.1. WES, Bioinformatic Analysis, and Filtering

An average of 81,170,229 million reads were output by the runs. Of these, 92.29% showed a Phred quality score > 30. After duplicate discard, an average of 75,411,435 reads were filtered and mapped to the GRCh38 human reference genome. The percentage of on-target reads was on average 71.57%, calculated on the deduplicated mapped read numbers. The quality report summary of each run is provided in Table S1. Regarding variant calling, a mean of 40,090 variants was annotated for each exome. Following the application of the above-mentioned filtering criteria, about 230 variants were selected for each sample. These included non-synonymous, nonsense, and frameshift mutations, whose reported minor allele frequency (MAF) was estimated to be < 0.01. Full lists are available in Table S2.

2.2. Gene Clustering and Prioritization

The ClueGO (Gene Ontology) enrichment analysis allowed to cluster the mutated genes for each exome in order to highlight the pathways they are involved in. In Table 1 only annotated terms showing the Bonferroni-adjusted p -value ≤ 0.05 were reported, both for each single term and for the entire cluster. The full lists are available in Table S3. Annotations related to cell adhesion (GO:1903392, GO:0051895, R-HSA:382054, GO:0038089, GO:0007157, GO:0120193, GO:1904886), cardiovascular development (WP:3668, GO:0003279, GO:0035904, GO:0060840, GO:0060976, GO:0060411), Notch signaling (GO:0007221, R-HSA:9021450, R-HSA:9013508, GO:0045747, WP:268, R-HSA:9012852), and TGF β R signaling (GO:1903846, GO:0030511) were highly represented in all the AVM samples. Furthermore, ontologies related to microtubule assembly and cell motility (GO:0003341, GO:0001578, GO:0001539, GO:0031122, GO:0060285) were also widely frequent. Interestingly, pathways related to ion conductance (GO:1904063, GO:0034766, GO:2001258, GO:0043267, GO:0016248, GO:0008200) were highly enriched in the AVM5 sample.

Table 1. ClueGO (Gene Ontology) enrichment analysis results.

Sample	GO ID	GO Term	Ontology Source	Term <i>p</i> -Value Corrected with Bonferroni Step Down	Group <i>p</i> -Value Corrected with Bonferroni Step Down	Associated Genes Found
AVM1	GO:0003341	cilium movement	GO_BiologicalProcess-EBI-UniProt-GOA_27.02.2019_00h00	0.00	0.00	(<i>ASPM, CFAP206, DNAH1, DNAH5, HYDIN, TEKT5</i>)
	GO:0035082	axoneme assembly	GO_BiologicalProcess-EBI-UniProt-GOA_27.02.2019_00h00	0.01	0.00	(<i>CFAP206, DNAH1, DNAH5, HYDIN, RP1L1</i>)
	R-HSA:2129379	molecules associated with elastic fibers	REACTOME_Pathways_27.02.2019	0.01	0.05	(<i>FBN2, FBN3, LTBP1, LTBP4</i>)
	GO:2000105	positive regulation of DNA-dependent DNA replication	GO_BiologicalProcess-EBI-UniProt-GOA_27.02.2019_00h00	0.01	0.14	(<i>CDC7, FLG, SYTL2</i>)
	GO:0097722	sperm motility	GO_BiologicalProcess-EBI-UniProt-GOA_27.02.2019_00h00	0.02	0.00	(<i>ASPM, CACNA11, DNAH1, DNAH5, SLC22A16, TEKT5</i>)
	R-HSA:1566948	elastic fiber formation	REACTOME_Pathways_27.02.2019	0.02	0.05	(<i>FBN2, FBN3, LTBP1, LTBP4</i>)
	GO:0030317	flagellated sperm motility	GO_BiologicalProcess-EBI-UniProt-GOA_27.02.2019_00h00	0.02	0.00	(<i>ASPM, CACNA11, DNAH1, DNAH5, SLC22A16, TEKT5</i>)
	GO:0018410	C-terminal protein amino acid modification	GO_BiologicalProcess-EBI-UniProt-GOA_27.02.2019_00h00	0.03	0.02	(<i>ASPM, LCMT2, SH2B1</i>)
	GO:0005044	scavenger receptor activity	GO_BiologicalProcess-EBI-UniProt-GOA_27.02.2019_00h00	0.03	0.03	(<i>LRP1, MEGF10, STAB1</i>)
	GO:1903078	positive regulation of protein localization to plasma membrane	GO_BiologicalProcess-EBI-UniProt-GOA_27.02.2019_00h00	0.03	0.03	(<i>CARD14, LRP1, NKD2</i>)
	WP:3668	hypothesized pathways in pathogenesis of cardiovascular disease	WikiPathways_27.02.2019	0.04	0.05	(<i>FBN2, FBN3, LTBP1</i>)
	GO:0001578	microtubule bundle formation	GO_BiologicalProcess-EBI-UniProt-GOA_27.02.2019_00h00	0.05	0.00	(<i>CFAP206, DNAH1, DNAH5, HYDIN, RP1L1</i>)
	GO:1903392	negative regulation of adherens junction organization	GO_BiologicalProcess-EBI-UniProt-GOA_27.02.2019_00h00	0.05	0.07	(<i>DLEC1, LRP1, TEPI1</i>)
	GO:0051895	negative regulation of focal adhesion assembly	GO_BiologicalProcess-EBI-UniProt-GOA_27.02.2019_00h00	0.05	0.07	(<i>DLEC1, LRP1, TEPI1</i>)
AVM2	GO:0031122	cytoplasmic microtubule organization	GO_BiologicalProcess-EBI-UniProt-GOA_27.02.2019_00h00	0.03	0.02	(<i>GOLGA4, KIF19, MBD1, PCMI, TUBGCP6</i>)
	GO:0042267	natural killer cell mediated cytotoxicity	GO_BiologicalProcess-EBI-UniProt-GOA_27.02.2019_00h00	0.03	0.08	(<i>LGALS9, LILRB1, PIK3R6</i>)
	GO:0070228	regulation of lymphocyte apoptotic process	GO_BiologicalProcess-EBI-UniProt-GOA_27.02.2019_00h00	0.03	0.09	(<i>IRS2, LGALS9, SLC39A10</i>)
	R-HSA:450346	activated human TAK1 phosphorylates MKK3/MKK6	REACTOME_Reactions_27.02.2019	0.04	0.00	(<i>MAP2K3, NOD1, TAB1</i>)

Table 1. Cont.

Sample	GO ID	GO Term	Ontology Source	Term <i>p</i> -Value Corrected with Bonferroni Step Down	Group <i>p</i> -Value Corrected with Bonferroni Step Down	Associated Genes Found
	GO:0061098	positive regulation of protein tyrosine kinase activity	GO_BiologicalProcess-EBI-UniProt-GOA_27.02.2019_00h00	0.05	0.02	(AGXT, DGKQ, DOK7, ERCC6, RELN)
R-HSA:450302		activated TAK1 mediates p38 MAPK activation	REACTOME_Pathways_27.02.2019	0.06	0.00	(MAP2K3, NOD1, TAB1)
R-HSA:448424		interleukin-17 signaling	REACTOME_Pathways_27.02.2019	0.06	0.00	(MAP2K3, NOD1, TAB1)
R-HSA:382054		PDGF binds to extracellular matrix proteins	REACTOME_Reactions_27.02.2019	0.07	0.04	(COL6A3, COL6A6, SPP1)
WP:231		TNF alpha signaling pathway	WikiPathways_27.02.2019	0.08	0.00	(KSR1, MAP2K3, NFKBIE, NSMAF, TAB1)
R-HSA:186797		signaling by PDGF	REACTOME_Pathways_27.02.2019	0.08	0.04	(COL6A3, COL6A6, GRB7, SPP1)
GO:0036498		IRE1-mediated unfolded protein response	GO_BiologicalProcess-EBI-UniProt-GOA_27.02.2019_00h00	0.08	0.04	(ARFGAP3, EXTL1, NR1H4, VAPB, WFS1)
GO:0035176		social behavior	GO_BiologicalProcess-EBI-UniProt-GOA_27.02.2019_00h00	0.09	0.02	(HTT, MBD1, PCM1)
R-HSA:373739		ankyrins link voltage-gated sodium and potassium channels to spectrin and L1 interaction between L1 and ankyrins	REACTOME_Reactions_27.02.2019	0.10	0.05	(ANK2, SCN7A, SPTA1)
R-HSA:445095		ankyrins	REACTOME_Pathways_27.02.2019	0.11	0.05	(ANK2, SCN7A, SPTA1)
GO:1901618		organic hydroxy compound transmembrane transporter activity	GO_BiologicalProcess-EBI-UniProt-GOA_27.02.2019_00h00	0.11	0.03	(AQP7, HTT, SLC10A6)
GO:0006890		retrograde vesicle-mediated transport, Golgi to endoplasmic reticulum	GO_BiologicalProcess-EBI-UniProt-GOA_27.02.2019_00h00	0.13	0.05	(ARFGAP3, CENPE, ERGIC1, HTT, TAPBP)
GO:0035036		sperm-egg recognition	GO_BiologicalProcess-EBI-UniProt-GOA_27.02.2019_00h00	0.13	0.05	(CATSPER2, ZAN, ZP1)
GO:0021846		cell proliferation in forebrain	GO_BiologicalProcess-EBI-UniProt-GOA_27.02.2019_00h00	0.13	0.02	(KIF14, MBD1, PCM1)
GO:0018195		peptidyl-arginine modification	GO_BiologicalProcess-EBI-UniProt-GOA_27.02.2019_00h00	0.13	0.05	(NR1H4, PADI2, PRMT7)
GO:0002753		cytoplasmic pattern recognition receptor signaling pathway	GO_BiologicalProcess-EBI-UniProt-GOA_27.02.2019_00h00	0.15	0.00	(ALPK1, DHX58, NOD1, TAB1)
R-HSA:6807875		ARFGAP, cargo, v-SNAREs, and p24 proteins bind nascent COPI complex	REACTOME_Reactions_27.02.2019	0.19	0.05	(ANK2, ARFGAP3, SPTA1)
R-HSA:6807877		ARFGAPs stimulate ARF GTPase activity	REACTOME_Reactions_27.02.2019	0.19	0.05	(ANK2, ARFGAP3, SPTA1)

Table 1. Cont.

Sample	GO ID	GO Term	Ontology Source	Term <i>p</i> -Value Corrected with Bonferroni Step Down	Group <i>p</i> -Value Corrected with Bonferroni Step Down	Associated Genes Found
	R-HSA:450294	MAP kinase activation	REACTOME_Pathways_27.02.2019	0.20	0.00	(MAP2K3, NOD1, TAB1)
	R-HSA:375165	NCAM signaling for neurite out-growth	REACTOME_Pathways_27.02.2019	0.22	0.04	(COL6A3, COL6A6, SPTA1)
	R-HSA:2022090	assembly of collagen fibrils and other multimeric structures	REACTOME_Pathways_27.02.2019	0.22	0.04	(COL6A3, COL6A6, LAMA3)
	R-HSA:168643	nucleotide-binding domain, leucine rich repeat containing receptor (NLR) signaling pathways	REACTOME_Pathways_27.02.2019	0.23	0.00	(NOD1, PSTPIP1, TAB1)
	GO:1903573	negative regulation of response to endoplasmic reticulum stress	GO_BiologicalProcess-EBI-UniProt-GOA_27.02.2019_00h00	0.23	0.04	(NR1H4, PRKN, WFS1)
AVM3	GO:0038089	positive regulation of cell migration by vascular endothelial growth factor signaling pathway	GO_BiologicalProcess-EBI-UniProt-GOA_27.02.2019_00h00	0.01	0.17	(KDR, MYO1C, PKD1)
	GO:0007157	heterophilic cell–cell adhesion via plasma membrane cell adhesion molecules	GO_BiologicalProcess-EBI-UniProt-GOA_27.02.2019_00h00	0.04	0.09	(HMCN1, RP9, SPG7)
	GO:0120193	tight junction organization	GO_BiologicalProcess-EBI-UniProt-GOA_27.02.2019_00h00	0.04	0.09	(EPHA2, MYO1C, PDZD4)
	GO:0032688	negative regulation of interferon-beta production	GO_BiologicalProcess-EBI-UniProt-GOA_27.02.2019_00h00	0.04	0.08	(LRRFIP1, MYO1C, NLRC3)
	GO:0048739	cardiac muscle fiber development	GO_BiologicalProcess-EBI-UniProt-GOA_27.02.2019_00h00	0.08	0.05	(MYOM2, OBSL1, SPG7)
AVM4	GO:0001539	cilium or flagellum-dependent cell motility	GO_BiologicalProcess-EBI-UniProt-GOA_27.02.2019_00h00	0.00	0.00	(DNAH11, DNAH14, DNAH2, DNAH3, DNAH8, GAS8)
	GO:0060285	cilium-dependent cell motility	GO_BiologicalProcess-EBI-UniProt-GOA_27.02.2019_00h00	0.00	0.00	(DNAH11, DNAH14, DNAH2, DNAH3, DNAH8, GAS8)
	GO:0007221	positive regulation of transcription of Notch receptor target	GO_BiologicalProcess-EBI-UniProt-GOA_27.02.2019_00h00	0.00	0.00	(MAML1, NOTCH3, OPN1LW, PLXND1, SPHKAP)
	WP:334	GPCRs, class B secretin-like	WikiPathways_27.02.2019	0.01	0.10	(ADCYAP1R1, ADGRG2, GLP2R, SCTR)
	GO:0003279	cardiac septum development	GO_BiologicalProcess-EBI-UniProt-GOA_27.02.2019_00h00	0.01	0.00	(CRELD1, DNAH11, LRP2, MAML1, PLXND1, SLIT2, SMO, TAB1)

Table 1. Cont.

Sample	GO ID	GO Term	Ontology Source	Term <i>p</i> -Value Corrected with Bonferroni Step Down	Group <i>p</i> -Value Corrected with Bonferroni Step Down	Associated Genes Found
	GO:0071503	response to heparin	GO_BiologicalProcess-EBI-UniProt-GOA_27.02.2019_00h00	0.02	0.01	(AOC1, GPIHBP1, SLIT2)
R-HSA:9021450		PLXND1 gene expression is stimulated by NOTCH1/NOTCH3 coactivator complexes	REACTOME_Reactions_27.02.2019	0.02	0.00	(MAML1, NOTCH3, PLXND1)
	GO:0061476	response to anticoagulant	GO_BiologicalProcess-EBI-UniProt-GOA_27.02.2019_00h00	0.03	0.01	(AOC1, GPIHBP1, SLIT2)
R-HSA:2162123		synthesis of prostaglandin (PG) and thromboxane (TX)	REACTOME_Pathways_27.02.2019	0.03	0.19	(AKR1C3, HPGD, TBXAS1)
	GO:0003205	cardiac chamber development	GO_BiologicalProcess-EBI-UniProt-GOA_27.02.2019_00h00	0.04	0.00	(CRELD1, DNAH11, LRP2, MAML1, PKD1, PLXND1, SLIT2, SMO, TAB1)
	GO:0048278	vesicle docking	GO_BiologicalProcess-EBI-UniProt-GOA_27.02.2019_00h00	0.05	0.15	(CTBP2, SCFD2, STX11)
	GO:0007157	heterophilic cell–cell adhesion via plasma membrane cell adhesion molecules	GO_BiologicalProcess-EBI-UniProt-GOA_27.02.2019_00h00	0.05	0.15	(FAT4, HMCN1, NUFIP2)
	GO:0021795	cerebral cortex cell migration	GO_BiologicalProcess-EBI-UniProt-GOA_27.02.2019_00h00	0.05	0.15	(SLIT2, SRGAP2, SUN1)
	GO:0002753	cytoplasmic pattern recognition receptor signaling pathway	GO_BiologicalProcess-EBI-UniProt-GOA_27.02.2019_00h00	0.05	0.25	(ALPK1, IRAK2, TAB1)
	GO:0007616	long-term memory	GO_BiologicalProcess-EBI-UniProt-GOA_27.02.2019_00h00	0.09	0.04	(CTNS, GRIA1, PJA2, PRNP)
	GO:0007613	memory	GO_BiologicalProcess-EBI-UniProt-GOA_27.02.2019_00h00	0.11	0.04	(ADGRF1, CHRN2, CIC, CTNS, GRIA1, PJA2, PRNP)
R-HSA:9013508		NOTCH3 intracellular domain regulates transcription	REACTOME_Pathways_27.02.2019	0.14	0.00	(MAML1, NOTCH3, PLXND1)
	GO:0035904	aorta development	GO_BiologicalProcess-EBI-UniProt-GOA_27.02.2019_00h00	0.25	0.00	(LRP2, PLXND1, TAB1)
	GO:0060840	artery development	GO_BiologicalProcess-EBI-UniProt-GOA_27.02.2019_00h00	0.25	0.00	(HPGD, LRP2, NOTCH3, PLXND1, TAB1)
	GO:0045747	positive regulation of Notch signaling pathway	GO_BiologicalProcess-EBI-UniProt-GOA_27.02.2019_00h00	0.27	0.00	(MAML1, NEPRO, OPN1LW, SPHKAP)
	GO:0035082	axoneme assembly	GO_BiologicalProcess-EBI-UniProt-GOA_27.02.2019_00h00	0.33	0.00	(DNAH8, GAS8, RSPH1)

Table 1. Cont.

Sample	GO ID	GO Term	Ontology Source	Term <i>p</i> -Value Corrected with Bonferroni Step Down	Group <i>p</i> -Value Corrected with Bonferroni Step Down	Associated Genes Found
	WP:268	Notch signaling	WikiPathways_27.02.2019	0.39	0.00	(CTBP2, MAML1, NOTCH3)
	GO:1903846	positive regulation of cellular response to transforming growth factor beta stimulus	GO_BiologicalProcess-EBI-UniProt-GOA_27.02.2019_00h00	0.40	0.00	(OPN1LW, RNF111, SPHKAP)
	GO:0030511	positive regulation of transforming growth factor beta receptor signaling pathway	GO_BiologicalProcess-EBI-UniProt-GOA_27.02.2019_00h00	0.40	0.00	(OPN1LW, RNF111, SPHKAP)
R-HSA:9012852		signalling by NOTCH3	REACTOME_Pathways_27.02.2019	0.41	0.00	(MAML1, NOTCH3, PLXND1)
	GO:0060976	coronary vasculature development	GO_BiologicalProcess-EBI-UniProt-GOA_27.02.2019_00h00	0.41	0.00	(LRP2, PLXND1, TAB1)
	GO:0060411	cardiac septum morphogenesis	GO_BiologicalProcess-EBI-UniProt-GOA_27.02.2019_00h00	0.42	0.00	(DNAH11, LRP2, SLIT2, SMO)
AVM5	WP:2572	primary focal segmental glomerulosclerosis (FSGS)	WikiPathways_27.02.2019	0.03	0.05	(AGRN, CAMK2B, LAMB2, LMX1B, MKI67)
	GO:0006027	glycosaminoglycan catabolic process	GO_BiologicalProcess-EBI-UniProt-GOA_27.02.2019_00h00	0.04	0.08	(AGRN, CD44, GPX4)
	GO:0031952	regulation of protein autophosphorylation	GO_BiologicalProcess-EBI-UniProt-GOA_27.02.2019_00h00	0.08	0.04	(CA5A, CAMK2B, ENG)
	GO:1904886	beta-catenin destruction complex disassembly	GO_BiologicalProcess-EBI-UniProt-GOA_27.02.2019_00h00	0.08	0.05	(AXIN1, CA5A, DVL1)
	GO:0097150	neuronal stem cell population maintenance	GO_BiologicalProcess-EBI-UniProt-GOA_27.02.2019_00h00	0.09	0.05	(BRCA2, FANCC, MBD1)
R-HSA:2142753		arachidonic acid metabolism	REACTOME_Pathways_27.02.2019	0.09	0.05	(CYP4B1, CYP4F3, GPX4, PRXL2B)
	GO:1904063	negative regulation of cation transmembrane transport	GO_BiologicalProcess-EBI-UniProt-GOA_27.02.2019_00h00	0.10	0.04	(ARHGEF40, CA5A, CAMK2B, EPHB2, KEL)
	GO:0007528	neuromuscular junction development	GO_BiologicalProcess-EBI-UniProt-GOA_27.02.2019_00h00	0.15	0.05	(AGRN, DVL1, LAMB2)
	GO:0034766	negative regulation of ion transmembrane transport	GO_BiologicalProcess-EBI-UniProt-GOA_27.02.2019_00h00	0.18	0.04	(ARHGEF40, CA5A, CAMK2B, EPHB2, KEL)
	GO:0043267	negative regulation of potassium ion transport	GO_BiologicalProcess-EBI-UniProt-GOA_27.02.2019_00h00	0.22	0.04	(CA5A, CPAMD8, KEL)
	GO:0044091	membrane biogenesis	GO_BiologicalProcess-EBI-UniProt-GOA_27.02.2019_00h00	0.25	0.04	(CA5A, EPHB2, PTPRH)

Table 1. Cont.

Sample	GO ID	GO Term	Ontology Source	Term <i>p</i> -Value Corrected with Bonferroni Step Down	Group <i>p</i> -Value Corrected with Bonferroni Step Down	Associated Genes Found
	GO:2001258	negative regulation of cation channel activity	GO_BiologicalProcess-EBI-UniProt-GOA_27.02.2019_00h00	0.26	0.04	(CA5A, CAMK2B, EPHB2)
	GO:0071709	membrane assembly	GO_BiologicalProcess-EBI-UniProt-GOA_27.02.2019_00h00	0.28	0.04	(CA5A, EPHB2, PTPRH)
	GO:0016248	channel inhibitor activity	GO_BiologicalProcess-EBI-UniProt-GOA_27.02.2019_00h00	0.28	0.04	(CA5A, CAMK2B, PHPT1)
	GO:0008200	ion channel inhibitor activity	GO_BiologicalProcess-EBI-UniProt-GOA_27.02.2019_00h00	0.28	0.04	(CA5A, CAMK2B, PHPT1)

The table reports annotations from ClueGO enrichment analysis. For each sample, the enriched pathways are mentioned as GO Term (3rd column) and the ontology sources (GeneOntology, WikiPathways, Reactome) are reported (4th column), as well as the clustered genes (7th column). Only annotations showing Bonferroni-adjusted *p*-value ≤ 0.05 for term or group (5th and 6th columns, respectively) are reported. Full results are available in Table S3. ARFGAP: Adenosine diphosphate Ribosylation Factor-GTPase; AVM: Arteriovenous malformation. The number (1–5) indicates the sample; COPI: coating protein 1; GPCR: G protein-coupled receptor; MAP: Mitogen-Activated Protein; MAPK: Mitogen-Activated Protein Kinase; MKK: MAP Kinase Kinase; NCAM: Neural Cell Adhesion Molecule; PDGF: Platelet Derived Growth Factor; PLXND1: Plexin D1; TAK1: TGF-Beta-Activated Kinase 1; TNF: Tumor Necrosis Factor; IRE1: Inositol-Requiring Protein 1; v-SNARE: Vesicle-Soluble NSF (N-Ethylmaleimide-Sensitive Factor) Attachment Protein Receptor.

The table reports annotations from ClueGO enrichment analysis. For each sample, the enriched pathways are mentioned as GO Term (3rd column) and the ontology sources (GeneOntology, WikiPathways, Reactome) are reported (4th column), as well as the clustered genes (7th column). Only annotations showing Bonferroni-adjusted p -value ≤ 0.05 for term or group (5th and 6th columns, respectively) are reported. Full results are available in Table S3. ARFGAP: Adenosine diphosphate Ribosylation Factor-GTPase; AVM: Arteriovenous malformation. The number (1–5) indicates the sample; COPI: coating protein 1; GPCR: G protein-coupled receptor; MAP: Mitogen-Activated Protein; MAPK: Mitogen-Activated Protein Kinase; MKK: MAP Kinase Kinase; NCAM: Neural Cell Adhesion Molecule; PDGF: Platelet Derived Growth Factor; PLXND1: Plexin D1; TAK1: TGF-Beta-Activated Kinase 1; TNF: Tumor Necrosis Factor; IRE1: Inositol-Requiring Protein 1; v-SNARE: Vesicle-Soluble NSF (N-Ethylmaleimide-Sensitive Factor) Attachment Protein Receptor. Gene prioritization aimed to relate selected loci with others, already linked to bAVM development. ToppGene output a full list of the Test Gene Set, ordered according to their overall p -value. For each gene, the overall p -value is calculated on the basis of the single p -value for each training parameter considered. Therefore, also in this case, only genes showing an overall p -value ≤ 0.05 were selected for each sample. Together with this criterion, “Gene Ontology (GO) biological process” annotations were considered as prioritized for the five AVM exomes. These are *LTBP4*, *LTBP1*, *LRP1*, and *FBN2* for AVM1; *TAB1*, *RELN*, and *MAP2K3* for AVM2; *KDR* and *EPHA2* for AVM3; *NOTCH3*, *PLXND1*, *TAB1*, *CTBP2*, *SLIT2*, *RNF111*, *MAML1*, and *CHRN2* for AVM4; and *AXIN1*, *EPHB2*, *DVL1*, and *CAMK2B* for AVM5 (Table 2). The complete lists with detailed statistical parameters as well as the annotations linking the prioritized genes to the training genes are available in Table S4.

Although prioritization analysis was quite exhaustive, further loci were considered. These added loci were selected as they are involved in vasculogenesis and carry missense and nonsense variants. In particular, they were *FLT4*, *NCoR2*, *CCN1*, and *GIMAP1* in the AVM2 sample; *NOTCH4* in AVM3; and *ENG* and *TGFR2* in AVM5. In particular, *ENG* and *TGFR2* are known to be highly linked to brain AVM and HHT development. *NCoR2* was affected by the novel nonsense variant c.2078G>T (p.Glu693Ter) (Ensembl Transcript ID: ENST00000405201.5). As a consequence, the mutated protein counts 692 amino acids rather than the 2514 amino acids of the wild-type one. The mutation was detected in a heterozygous condition and resulted as “Damaging” and “Disease causing” in SIFT (<https://sift.bii.a-star.edu.sg/>) [9] and MutationTaster (<http://www.mutationtaster.org/>) [10] prediction tools, respectively (not shown).

2.3. Sanger Validation

Table 3 lists the variants detected in the genes previously prioritized. All these variants were confirmed by Sanger sequencing and were not detected in our internal 10 control exomes obtained from healthy subjects. Figure 1 reports only the electropherogram of the novel nonsense variant, c.2078G>T (p.Glu693Ter) affecting the *NCoR2* locus.

Table 2. Genes prioritized by ToppGene tool.

Ontology	Feature	ID	Name	Genes		
<i>GO: Biological Process</i>	Vessel development	GO:0001525	Angiogenesis	ACVRL1 ENG EPHA2 EPHB2 GDF2 KDR NOTCH3 PLXND1 SLIT2 TGFBR2		
		GO:0001568	Blood vessel development	ACVRL1 ENG EPHA2 EPHB2 GDF2 KDR PKD1 LRP1 LTBP1 TAB1 HPGD LRP2 NOTCH3 PLXND1 SLIT2 SMO TGFBR2		
		GO:0001569	Branching involved in blood vessel morphogenesis	GO:0001570	Vasculogenesis	ENG GDF2 PLXND1 TGFBR2 ENG EPHA2 GDF2 SMO KDR TGFBR2
		GO:0001944		Vasculature development	ACVRL1 ENG EPHA2 GDF2 KDR PKD1 LRP1 LTBP1 HPGD LRP2 NOTCH3 PLXND1 SLIT2 SMO TAB1 TGFBR2	
		GO:0048514	Blood vessel morphogenesis	ACVRL1 ENG EPHA2 EPHB2 GDF2 LRP1 KDR HPGD LRP2 NOTCH3 PLXND1 SLIT2 SMO TGFBR2		
		GO:1901342	Regulation of vasculature development	ACVRL1 ENG EPHA2 GDF2 KDR PLXND1 TGFBR2		
	TGFBR signaling	GO:0007179	Transforming growth factor beta receptor signaling pathway	ACVRL1 AXIN1 ENG FBN2 GDF2 LTBP1 LTBP4 HPGD RNF111 SMAD4 TAB1 TGFBR2		
		GO:0017015	Regulation of transforming growth factor beta receptor signaling pathway	AXIN1 ENG FBN2 GDF2 LTBP1 LTBP4 RNF111 SMAD4 TGFBR2		
		GO:0071559	Response to transforming growth factor beta	ACVRL1 AXIN1 ENG FBN2 GDF2 HPGD RNF111 LTBP1 LTBP4 SMAD4 TAB1 TGFBR2		
		GO:0071560	Cellular response to transforming growth factor beta stimulus	ACVRL1 AXIN1 ENG FBN2 GDF2 LTBP1 LTBP4 HPGD RNF111 SMAD4 TAB1 TGFBR2		
		GO:1903844	Regulation of cellular response to transforming growth factor beta stimulus	AXIN1 ENG FBN2 GDF2 LTBP1 LTBP4 SMAD4 TGFBR2		
	Heart development	GO:0003007	Heart morphogenesis	ACVRL1 DNAH11 ENG SMAD4 FAT4 LRP2 PLXND1 SLIT2 SMAD4 SMO TAB1 TGFBR2		
		GO:0003205	Cardiac chamber development	DNAH11 ENG LRP2 MAML1 PLXND1 SLIT2 LRP1 LTBP1 SMAD4 SMO TAB1 TGFBR2		
		GO:0003206	Cardiac chamber morphogenesis	DNAH11 ENG LRP2 SLIT2 SMAD4 SMO TGFBR2		
		GO:0003208	Cardiac ventricle morphogenesis	ENG LRP2 SMAD4 TGFBR2		
		GO:0003231	Cardiac ventricle development	ENG LTBP1 LRP2 SLIT2 SMAD4 TGFBR2		
		GO:0003279	Cardiac septum development	DNAH11 ENG LRP1 LTBP1 LRP2 MAML1 PLXND1 SLIT2 SMAD4 SMO TAB1 TGFBR2		
		GO:0007507	Heart development	ACVRL1 DNAH5 DNAH11 DVL1 ENG KDR PKD1 LRP1 LTBP1 FAT4 LRP2 MAML1 PLXND1 SLIT2 SMAD4 SMO TAB1 TGFBR2		
		GO:0060411	Cardiac septum morphogenesis	DNAH11 ENG LRP2 SLIT2 SMAD4 SMO TGFBR2		
		GO:0072358	Cardiovascular system development	ACVRL1 ENG EPHA2 EPHB2 GDF2 KDR PKD1 LRP1 LTBP1 HPGD LRP2 NOTCH3 PLXND1 SLIT2 SMO TAB1 TGFBR2		
		GO:0072359	Circulatory system development	ACVRL1 DNAH5 DNAH11 DVL1 ENG EPHA2 EPHB2 FAT4 GDF2 LRP1 LTBP1 KDR PKD1 HPGD LRP2 MAML1 NOTCH3 PLXND1 SLIT2 SMAD4 SMO TAB1 TGFBR2		
	GO:2000826	Regulation of heart morphogenesis	ENG SMAD4 SMO TGFBR2			
	BMP signaling	GO:0030509	BMP signaling pathway	ACVRL1 ENG GDF2 KDR LRP2 SMAD4		
		GO:0030510	Regulation of BMP signaling pathway	ACVRL1 ENG GDF2 KDR LRP2 SMAD4		
		GO:0030513	Positive regulation of BMP signaling pathway	ACVRL1 ENG GDF2 KDR SMAD4		
		GO:0071772	Response to BMP	ACVRL1 ENG GDF2 KDR LRP2 SMAD4		
		GO:0071773	Cellular response to BMP stimulus	ACVRL1 ENG GDF2 KDR LRP2 SMAD4		
Endothelial/mesenchymal differentiation	GO:0001935	Endothelial cell proliferation	ACVRL1 ENG EPHA2 GDF2 KDR			
	GO:0001936	Regulation of endothelial cell proliferation	ACVRL1 ENG GDF2 KDR			
	GO:0003158	Endothelium development	ACVRL1 ENG GDF2 KDR SMAD4			
	GO:0045446	Endothelial cell differentiation	ACVRL1 ENG GDF2 KDR SMAD4			
	GO:0048762	Mesenchymal cell differentiation	ACVRL1 ENG SMAD4 SMO TGFBR2			
	GO:0060485	Mesenchyme development	ACVRL1 ENG SMAD4 SMO TGFBR2			

Table 2. Cont.

Ontology	Feature	ID	Name	Genes
GO: Biological Process	Hypoxia response	GO:0001666	Response to hypoxia	<i>ACVRL1</i> <i>CHRN2</i> <i>ENG</i> <i>KDR</i> <i>SMAD4</i> <i>TGFBR2</i>
		GO:0036293	Response to decreased oxygen levels	<i>ACVRL1</i> <i>CHRN2</i> <i>ENG</i> <i>KDR</i> <i>SMAD4</i> <i>TGFBR2</i>
		GO:0070482	Response to oxygen levels	<i>ACVRL1</i> <i>CHRN2</i> <i>ENG</i> <i>KDR</i> <i>SMAD4</i> <i>TGFBR2</i>
Human Phenotype	Cerebrovascular malformations	HP:0100026	Arteriovenous malformation	<i>ACVRL1</i> <i>BRCA2</i> <i>DVL1</i> <i>ENG</i> <i>FANCC</i> <i>GDF2</i> <i>SMAD4</i>
		HP:0001009	Telangiectasia	<i>ACVRL1</i> <i>BRCA2</i> <i>ENG</i> <i>FANCC</i> <i>GDF2</i> <i>SMAD4</i>
		HP:0001048	Cavernous hemangioma	<i>ACVRL1</i> <i>AXIN1</i> <i>ENG</i> <i>GDF2</i> <i>SMAD4</i>
	Benign/malignant neoplasm	HP:0005306	Capillary hemangioma	<i>ACVRL1</i> <i>DVL1</i> <i>ENG</i> <i>GDF2</i> <i>KDR</i> <i>SMAD4</i>
		HP:0001028	Hemangioma	<i>ACVRL1</i> <i>AXIN1</i> <i>DVL1</i> <i>ENG</i> <i>GDF2</i> <i>KDR</i> <i>PRKN</i> <i>SMAD4</i>
		HP:0100742	Vascular neoplasm	<i>ACVRL1</i> <i>AXIN1</i> <i>DVL1</i> <i>ENG</i> <i>GDF2</i> <i>KDR</i> <i>PRKN</i> <i>SMAD4</i>
	Vessel dilatation	HP:0002624	Abnormal venous morphology	<i>ACVRL1</i> <i>AXIN1</i> <i>BRCA2</i> <i>ENG</i> <i>EPHB2</i> <i>GDF2</i> <i>NOTCH3</i> <i>SMAD4</i>
		HP:0002619	Varicose veins	<i>ACVRL1</i> <i>AXIN1</i> <i>ENG</i> <i>GDF2</i> <i>NOTCH3</i> <i>SMAD4</i>
		HP:0004414	Abnormality of the pulmonary artery	<i>ACVRL1</i> <i>ENG</i> <i>FBN2</i> <i>GDF2</i> <i>LTBP4</i> <i>SMAD4</i> <i>TGFBR2</i>
		HP:0004930	Abnormality of the pulmonary vasculature	<i>ACVRL1</i> <i>AXIN1</i> <i>ENG</i> <i>FBN2</i> <i>GDF2</i> <i>LTBP4</i> <i>SMAD4</i> <i>TGFBR2</i>
HP:0100659		Abnormality of the cerebral vasculature	<i>ACVRL1</i> <i>BRCA2</i> <i>ENG</i> <i>GDF2</i> <i>NOTCH3</i> <i>PKD1</i> <i>PRNP</i> <i>SMAD4</i> <i>SMO</i> <i>TGFBR2</i> <i>WFS1</i>	
HP:0009145	Abnormal cerebral artery morphology	<i>ACVRL1</i> <i>BRCA2</i> <i>ENG</i> <i>FANCC</i> <i>GDF2</i> <i>NOTCH3</i> <i>PKD1</i> <i>SMAD4</i> <i>TGFBR2</i>		
HP:0011004	Abnormal systemic arterial morphology	<i>ACVRL1</i> <i>DNAH11</i> <i>ENG</i> <i>FBN2</i> <i>GDF2</i> <i>NOTCH3</i> <i>PKD1</i> <i>SMAD4</i> <i>TGFBR2</i>		
Mouse Phenotype	Cerebrovascular malformations	MP:0006093	Arteriovenous malformation	<i>ACVRL1</i> <i>ENG</i> <i>GDF2</i> <i>NOTCH3</i>
		MP:0000259	Abnormal vascular development	<i>ACVRL1</i> <i>CD44</i> <i>CTBP2</i> <i>ENG</i> <i>EPHA2</i> <i>KDR</i> <i>HPGD</i> <i>MAML1</i> <i>NOTCH3</i> <i>PLXND1</i> <i>LTBP1</i> <i>SMAD4</i> <i>SMO</i> <i>SPP1</i> <i>TGFBR2</i>
	Vessel dilatation	MP:0001614	Abnormal blood vessel morphology	<i>ACVRL1</i> <i>CD44</i> <i>CTBP2</i> <i>DNAH11</i> <i>DNAH5</i> <i>ENG</i> <i>EPHA2</i> <i>FBN2</i> <i>GDF2</i> <i>KDR</i> <i>PKD1</i> <i>LMX1B</i> <i>LRP1</i> <i>LTBP1</i> <i>LTBP4</i> <i>HPGD</i> <i>LRP2</i> <i>MAML1</i> <i>NOTCH3</i> <i>PLXND1</i> <i>SLIT2</i> <i>NR1H4</i> <i>SMAD4</i> <i>SPP1</i> <i>TAB1</i> <i>TGFBR2</i>
		MP:0003410	Abnormal artery development	<i>ACVRL1</i> <i>ENG</i> <i>NOTCH3</i> <i>PLXND1</i> <i>SMO</i> <i>KDR</i> <i>LTBP1</i> <i>TGFBR2</i>
		MP:0004787	Abnormal dorsal aorta morphology	<i>ACVRL1</i> <i>ENG</i> <i>KDR</i> <i>TGFBR2</i>
	MP:0000267	Abnormal heart development	<i>ACVRL1</i> <i>AXIN1</i> <i>CTBP2</i> <i>DNAH5</i> <i>ENG</i> <i>KDR</i> <i>MAML1</i> <i>PKD1</i> <i>SMAD4</i> <i>SMO</i> <i>TGFBR2</i>	
	Defects in embryo vasculogenesis	MP:0001719	Absent vitelline blood vessels	<i>ACVRL1</i> <i>CTBP2</i> <i>ENG</i> <i>KDR</i> <i>SMO</i> <i>TGFBR2</i>
MP:0003229		Abnormal vitelline vasculature morphology	<i>ACVRL1</i> <i>CTBP2</i> <i>ENG</i> <i>KDR</i> <i>SMO</i> <i>SMAD4</i> <i>TGFBR2</i>	
Disease	Cerebrovascular malformations	C0003857	Congenital arteriovenous malformation	<i>ACVRL1</i> <i>ENG</i> <i>NOTCH3</i> <i>SMAD4</i>
		C0334533	Arteriovenous hemangioma	<i>ACVRL1</i> <i>ENG</i> <i>NOTCH3</i> <i>SMAD4</i>
	Vessel disorders	C0007820	Cerebrovascular Disorders	<i>ACVRL1</i> <i>ENG</i> <i>GDF2</i> <i>NOTCH3</i> <i>PKD1</i> <i>RELN</i> <i>SMAD4</i> <i>SPP1</i> <i>TGFBR2</i>
		C0042373	Vascular Diseases	<i>ACVRL1</i> <i>ENG</i> <i>KDR</i> <i>NOTCH3</i> <i>PRKN</i> <i>SMAD4</i> <i>SPP1</i> <i>TGFBR2</i>
		C0002940	Aneurysm	<i>ACVRL1</i> <i>ENG</i> <i>LRP1</i> <i>LTBP4</i> <i>PKD1</i> <i>TGFBR2</i>

The table reports results obtained by ToppGene prioritization analysis giving as Training Gene Set *ACVRL1*, *ENG*, *GDF2*, *SMAD4*, and *TGFBR2*. According to the specific ontology, prioritized genes are shown in bold. Results are here summarized and grouped in relation to annotations. Data obtained for the single patient are available in Table S4. BMP: Bone Morphogenetic Protein; TGFBR: Transforming Growth Factor Beta Receptor.

Table 3. Variants affecting prioritized genes.

Locus	Gene	HGNC ID	SNP ID	Ensembl Transcript ID	Coding Sequence Change	Ensembl Protein ID	Protein Sequence Change
1p22.3	<i>CCN1</i> *	2654	rs765069158	ENST00000451137	c.G463C	ENSP00000398736	p.Gly155Arg
1p36.12	<i>EPHB2</i>	3393	rs142113032	ENST00000400191	c.847G>C	ENSP00000383053	p.Asp283His
1p36.13	<i>EPHA2</i>	3386	rs35484156	ENST00000358432	c.830C>T	ENSP00000351209	p.Ser277Leu
1p36.33	<i>DVL1</i>	3084	rs61735963	ENST00000378891	c.469G>A	ENSP00000368169	p.Ala157Thr
1q21.3	<i>CHRNA2</i>	1962	rs55685423	ENST00000368476	c.1191G>C	ENSP00000357461	p.Gln397His
2p22.3	<i>LTBP1</i>	6714	rs80163321 rs149319598	ENST00000404816	c. 2248 G>A c. 2410C>T	ENSP00000386043	p.Val750Ile p.Pro804Ser
3p24.1	<i>TGFBR2</i> *	11773	rs35766612	ENST00000295754	c.1159G>T	ENSP00000295754	p.Val387Leu
3q22.1	<i>PLXND1</i>	9107	rs137955512	ENST00000324093	c.2275C>T	ENSP00000317128	p.Pro759Ser
4p15.31	<i>SLIT2</i>	11086	rs115629108	ENST00000504154	c.4049G>A	ENSP00000422591	p.Ser1350Asn
4q12	<i>KDR</i>	6307	rs755067067	ENST00000263923	c.1990C>T	ENSP00000263923	p.Arg664Cys
5q23.3	<i>FBN2</i>	3604	rs28763954	ENST00000262464	c.976C>T	ENSP00000262464	p.Pro326Ser
5q35.3	<i>MAML1</i>	13632	rs113636707	ENST00000292599	c.569G>A	ENSP00000292599	p.Arg190His
5q35.3	<i>FLT4</i> *	3767	rs200763913	ENST00000261937	c.1133G>A	ENSP00000261937	p.Arg378His
6p21.32	<i>NOTCH4</i> *	7884	rs8192573	ENST00000375023	c.4037G>A	ENSP00000364163	p.Arg1346Gln
7p13	<i>CAMK2B</i>	1461	rs528355050	ENST00000395749	c.1577C>T	ENSP00000379098	p.Pro526Leu
7q22.1	<i>RELN</i>	9957	rs114684479 rs79499902	ENST00000428762	c.3477C>A c.5284G>A	ENSP00000392423	p.Asn1159Lys p.Val1762Ile
7q36.1	<i>GIMAP1</i> *	23237	rs1326399257	ENST00000307194	c.699G>A	ENSP00000302833	p.W233X
9q34.11	<i>ENG</i> *	3349	rs139398993	ENST00000373203	c.392C>T	ENSP00000362299	p.Pro131Leu
10q26.13	<i>CTBP2</i>	2595	rs1058301	ENST00000334808	c.387C>G	ENSP00000357816	p.Asp129Glu
12q13.3	<i>LRP1</i>	6692	rs113379328	ENST00000243077	c.7636G>A	ENSP00000243077	p.Gly2546Ser
12q24.31	<i>NCoR2</i> *	7673	Novel	ENST00000405201	c..2078G>T	ENSP00000384018	p.Glu693Ter
15q22.1-q22.2	<i>RNF111</i>	17384	rs142916216	ENST00000557998	c.888T>G	ENSP00000452732	p.Ile296Met
16p13.3	<i>AXIN1</i>	903	rs200741961	ENST00000262320	c.644C>T	ENSP00000262320	p.Ser215Leu
17p11.2	<i>MAP2K3</i>	6843	rs33911218 rs36047035	ENST00000342679	c.118C>G c.164G>C	ENSP00000345083	p.Pro40Ala p.Arg55Thr
19p13.12	<i>NOTCH3</i>	7883	rs141320511	ENST00000263388	c.4552C>A	ENSP00000263388	p.Leu1518Met
19q13.2	<i>LTBP4</i>	6717	rs35809725	ENST00000308370	c.4499A>T c.19A>C c.560G>A	ENSP00000311905	p.Tyr1500Phe
22q13.1	<i>TAB1</i>	18157	rs536084162 rs140879164	ENST00000216160	c.19A>C c.560G>A	ENSP00000216160	p.Ser7Arg p.Arg187His

For each variant, chromosomal band, gene name, HUGO Gene Nomenclature Committee gene name, variant ID, transcript and protein reference IDs of the Ensembl Genome Browser, coding sequence, and amino acid position changes are reported. * Loci not output by the ToppGene tool.

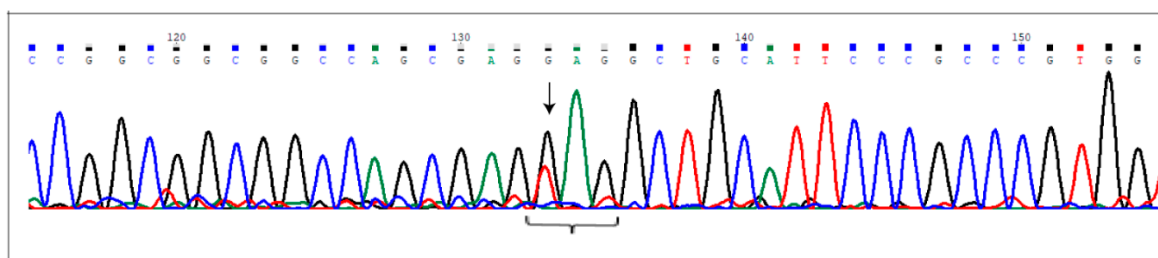


Figure 1. The c.2078G>T (p.Glu693Ter) at the *NCoR2* locus. Electropherogram shows the novel nonsense mutation affecting the *NCoR2* gene, detected in heterozygous condition in AVM2 sample. Nucleotide substitution is indicated by the arrow. The brace indicates the DNA sequence corresponding to the triplet carrying the mutated nucleotide (the first one).

3. Discussion

The genetic landscape of bAVM is to date quite elusive probably due to the very low frequency of inherited cases. Most patients are affected by sporadic forms whose molecular causes are waiting to be clarified. In many cases, lesions are congenital, increasing in size over the years until they become symptomatic. Due to the dynamic nature of bAVM and its high recidivism rate, it is well accepted that lesions arise as a consequence of continuous endogenous stimuli, as inherited and de novo genetic variants or epigenetic modifications occurring during embryo development [11,12]. Therefore, we performed WES analysis on a group of five patients affected by sporadic bAVM, highlighting the main pathways enriched by germline mutated genes. Despite mutated genes differing among patients, the pathways in which they converge are the same. Firstly, we checked for variants in *ENG*, *NOTCH4*, and *TGFβR2* that are known to be involved in arteriovenous malformation development [13,14]. Then, we searched for *KRAS* c.35G>T (p.Gly12Val) that was recurrently detected in bAVM patients [15] and none of them carried the mutation, as well as other variants within the gene. However, this was expected as our analysis was performed on DNA purified by peripheral blood. Mosaic-activating *KRAS* mutations, indeed, were found in sporadic AVM-derived specimens [16,17].

The ClueGO enrichment analysis revealed pathways related to microtubule formation, cell adhesion, and vascular remodeling as being highly enriched (Table 1). Moreover, prioritization analysis was performed for each sample to detect the main genes involved in TGFβR transduction pathways and, therefore, more likely associated to bAVM onset. As reported in Table S4a,b, several loci are noteworthy of consideration and the most relevant are listed in Table 2. However, among prioritized genes, here we briefly discuss those more likely related to bAVM development, in relation to the single sample. This selection was made considering significant *p*-values related to phenotypes and pathway, outputted by the ToppGene tool (Table S4a).

3.1. AVM1

Regarding AVM1, we focused on *LTBP1*, *LTBP4*, *FBN2*, and *LRP1* loci. *FBN2*, encoding for Fibrillin 2, and *LTBP1* and *LTBP4* belonging to the “latent transforming growth factor beta binding proteins” family, are ligands of TGF-β receptors [18,19]. With regard to *LRP1*, encoding for the LDL receptor related protein 1, expression data showed it is expressed in brain endothelial cells where it contributes to chemotactic cell migration, inducing sphingosine-1-phosphate proangiogenic signaling [20]. Moreover, depletion of *LRP1* determines defects of both large and small vessel morphogenesis leading to a lethal phenotype [21].

3.2. AVM2

Regarding data obtained from AVM2 exome, we considered variants affecting *TAB1*, *FLT4*, *RELN*, *MAP2K3*, *CCN1*, *GIMAP1*, and *NCoR2* loci. *TAB1* encodes for the TGF-β activated kinase 1 binding protein 1 and increases endothelial permeability, mediated by the non-canonical TGF-β

pathway following inflammation stimuli [22]. Moreover, TAB1 activates the TAK1 kinase, an upstream modulator of the p38 MAPK signaling. *MAP2K3* is also involved [23] in the same pathway and, in particular, a physical interaction between TAK1 and MAP2K3 has been reported [24]. Involvement of inflammatory response in bAVM is, to date, well accepted [25,26] and in this context, we detected a nonsense mutation, the c.699G>A (p.Trp233Ter) in *GIMAP1* gene. Together with the TGF β R2 signaling, Notch transduction pathways were also reported as promoting AVM development [27]. Therefore, we also considered prioritizing the *NCor2* locus, encoding for nuclear receptor co-repressor. We found the novel nonsense mutation, c.2078G>T (p.Glu693Ter) (Figure 1). *FLT4*, instead, encodes for the vascular endothelial growth factor receptor 3 (VEGFR3) [28]. Finally, we considered *CCN1* locus, encoding for the cellular communication network factor 1. Its expression is increased in the extracellular matrix surrounding microvessels and is growth factor-inducible. The protein promotes integrin-mediated endothelial cell adhesion in response to mechanotransduction signaling [29]. This evidence is well congruent with bAVM pathogenesis due to frequent insult by the high blood pressure within the lesions.

3.3. AVM3

Together with *NOTCH4*, variants carried by *EPHA2*, *EPHB4*, and *KDR* were detected in sample AVM3. *EPHA2* and *EPHB2* encode for two proteins belonging to the ephrin family, a subgroup of protein-tyrosine kinase receptors. Ephrins are vessel differentiation markers and their role is pivotal during early vasculogenesis. In particular, mesenchymal cells express *EPHB2*, a feature of arterial morphogenesis. A model proposed by Adams et al. hypothesizes interaction among type-B ephrins differentially expressed in arteries and veins as the basis of a remodeling process that leads to sprouting and capillary network development [30]. *EPHB2* expression is upregulated in capillaries during inflammation. This results in increased endothelial permeability and loss of vessel differentiation [31]. The absence of EphA2, instead, was shown to impair the blood–brain barrier, resulting in inhibition of endothelial cell migration and in enhancement of tight junction formation in human brain microvascular endothelial cells (HBMECs) [32]. *KDR* encodes for the vascular VEGFR2, essential for the organization of the embryonic vasculature and angiogenic sprouting [33].

3.4. AVM4

The highest number of prioritized genes was in the AVM4 sample. GO annotations for biological process revealed involvement in vasculature morphogenesis for *NOTCH3*, *PLXND1*, *SLIT2*, and *MAML1* loci. At the embryo stage, VEGF and Notch transduction signaling modulates *PLXND1* expression to guide organ vasculogenesis by promoting endothelial cell migration and proliferation [34]. In adults, instead, *PLXND1* expression is physiologically low and limited to a few cell types, such as endothelial cells [35]. Balancing effects on migration were reported for *SLIT2* [36]. *MAML1* is described as a NOTCH coactivator, even if its role in angiogenesis needs more elucidation [37]. Regarding the TGF- β /BMP pathway, we focused on the *RNF111* gene, encoding for the E3 ubiquitin-protein ligase. One of its targets is the SMAD7 protein that acts by inhibiting TGF- β /BMP signaling. Therefore, RNF111 activity is required to promote SMAD7 degradation and to enhance the TGF- β /BMP pathway [38]. TGF- β signaling is also upregulated by increased levels of CTBP2 (C-terminal binding protein 2), driving endothelial-to-mesenchymal transition (EMT) [39]. This gene was also mutated in the AVM4 patient. In the end, we focused our attention on the GO terms regarding the response to hypoxia (GO:0001666, GO:0036293, GO:0070482) with the patient as a carrier of rs55685423 (c.1191G>C, p.Gln397His) in the *CHRNA2* locus. This gene encodes for the cholinergic receptor nicotinic beta 2 subunit [40]. Its expression was demonstrated in HBMECs, where it contributes to capillary network formation and to angiogenic response to inflammation [41]. Notably, the same ontologies were also found in the AVM3 patient, annotated by the *KDR* locus.

3.5. AVM5

Finally, in the AVM5 sample we identified two variants in *ENG* and *TGFBR2* loci, rs139398993 (c.392C>T, p.Pro131Leu) and rs35766612 (c.1159G>T, p.Val387Leu), respectively. Moreover, *EPHB2* was also affected by a missense variant. Based on human and mouse phenotype ontologies, *DVL1* and *AXIN1* were annotated to the “cerebrovascular disease” term and, in particular, with AVM and telangiectasia phenotypes. *DVL1* is known to control postnatal angiogenesis [42]. *AXIN1* encodes for a negative regulator of the Wnt pathway, also enhancing TGF- β signaling by promoting the degradation of the inhibitory SMAD7, in a RNF111-dependent manner [43]. Surprisingly, it was recently described as an important regulator of embryo central nervous system (CNS) angiogenesis, and overexpression leads to premature vascular regression, followed by progressive dilation and inhibition of vascular maturation [44].

3.6. Novel Insights

Together with TGF- β /Notch signaling, GO annotations derived from the ClueGO enrichment analysis (Table 1) highlight a relevant presence of ontologies related to microtubule and cilia organization (GO:0003341, GO:0001578, GO:0031122, GO:0001539, GO:0060285). A recent study demonstrated that cilia are widely represented in endothelial cells during early vasculogenesis and in the later stages as vessel bifurcation point anastomosis. Zebrafish knock-down for cilia biogenesis gene models showed cilia disassembly following shear stress, resulting in remodeling of endothelial cell architecture and increased permeability and hemorrhagic events. Moreover, hemorrhages were only observed in head vasculature and were not observed in the trunk or caudal vessels [45]. Based on this evidence, germline defects in genes controlling cilia assembly might also contribute to brain AVM development as the result of mechanical stress induced by high blood flow and pressure. Clearly, this hypothesis needs to be adequately validated.

Another important property of the blood–brain barrier is the highly selective control of solute transport which is maintained by the exact spatial distribution of membrane transporters and ion channels. Polarization is a key factor for morpho-functional homeostasis of endothelial cells and was shown to be driven by VEGF via Ca²⁺ specific signaling pathways [46]. Moreover, dysregulation of K⁺ ion influx in non-excitabile cells was shown to lead to hyperpolarization of membrane potential with consequent increased intracellular Ca²⁺. This results in enhancement of cell proliferation and was also demonstrated in brain capillary endothelial cells [47]. However, if physiological Ca²⁺ concentration is abnormally excessive, endothelial cells undergo apoptosis [48]. Therefore, we focused attention on GO terms from the ClueGO analysis of sample AVM5. As shown in Table 1, GO terms related to transmembrane ion transport (GO:1904063, GO:0034766, GO:2001258, GO:0043267, GO:0016248, GO:0008200) are largely enriched, as well as those related to membrane biogenesis (GO:0044091, GO:0071709, GO:1904886) making the hypothesis of misregulation in bAVM onset conceivable.

Although these are preliminary findings, they are in accordance with what was recently published by Hauer and colleagues. They describe dysregulated expression of genes also involving cytoskeleton network and transmembrane transport in bAVM-derived specimens, when compared to intracranial control arteries [49]. Therefore, these results allow to elicit other mechanisms in pathogenesis of bAVM not only confined to the canonical TGF β R2 pathway.

3.7. Final Considerations

We discussed loci affected by germline variants in five bAVM samples. Despite these loci differing among the samples, they converged in regulation of the same cellular signaling pathways. This interconnection is represented in Figure 2. The image was obtained by STRING tool Version 11.0 (<https://string-db.org/>) [50]. Details on nodes and edges are supplied in Table S5.

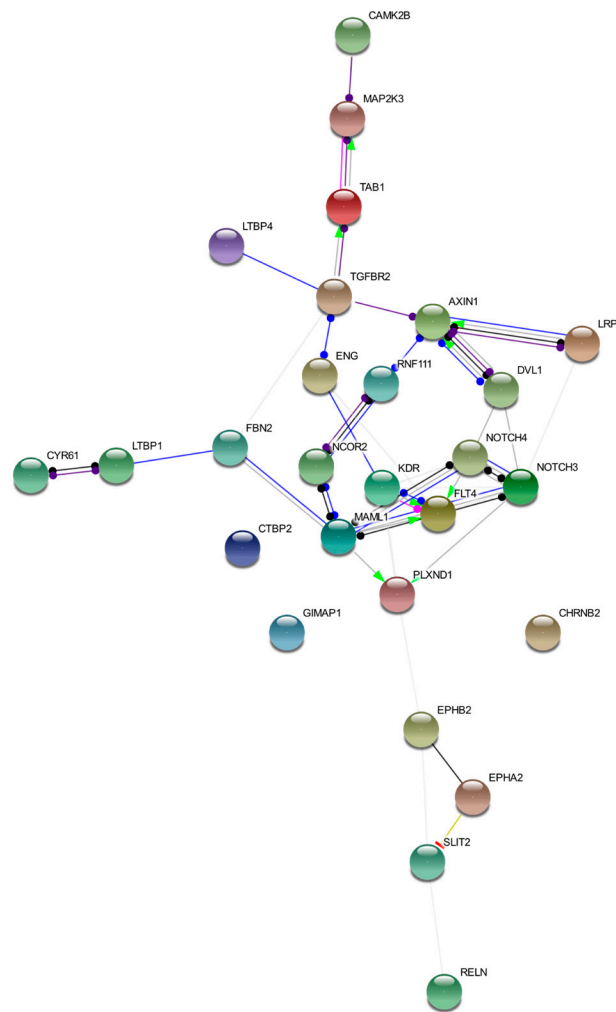


Figure 2. Functional network of prioritized genes. The image describes observed and inferred functional interactions linking prioritized genes. Nodes represent input proteins while edges represent protein–protein associations. Each edge color indicates a specific annotation. Green: activation; red: inhibition; blue: binding; light blue: phenotype; black: reaction; violet: catalysis; pink: posttranslational modification; yellow: transcriptional regulation.

According to prioritized genes, our data support findings previously reported [51,52] and, in particular, the genetic heterogeneity of the disease. These results suggest that sporadic bAVM is probably not a monogenic condition, rather it arises during early vasculogenesis at the embryo stage. In particular, following fertilization, the combination of both inherited and eventually de novo genetic variants in numerous loci controlling vessel development could result in early vasculogenesis impairment and lesion onset. However, the evidence that these patients develop lesions only in the CNS underlines the importance of the cross-talk between glial cells and endothelium during neurodevelopment and blood–brain barrier morphogenesis. Most genes considered here show an early peculiar expression in neural progenitor cells that contributes to correct vasculogenesis and angiogenetic processes. In this context, proteins related to axon guidance such as Slits, plexins, and ephrins are exhaustive examples [53,54]. However, a last consideration regards genes involved in DNA repair such as *WRN*, *FANCC*, *BRCA2*, *TP53BP1*, and others carrying rare missense variants. These variants might cause protein functional alteration and, subsequently, DNA repair impairment. At the embryo stage, this might trigger DNA errors resulting in somatic mutations. Clearly, as our study focused on germline variants, the role of somatic mutations is not evaluated here.

Germline genetic variants are endogenous and permanent factors affecting both early vasculogenesis and late angiogenesis. Endothelial remodeling is a continuous phenomenon, and this can explain the increased recidivism rate of bAVM. Therefore, our hypothesis regards the possibility of considering bAVM as the result of the co-existence of numerous low-penetrance loci controlling different processes during endothelial cell differentiation and maturation. This idea is supported by two observations. We selected only loci affected by rare variants (MAF < 0.01) and then, those most likely related to rare disease onset. Rare variants at the same loci were searched for in our internal 10 control exomes obtained from healthy subjects and none was detected.

Clearly, the main limitation of the study is related to the few samples considered and, certainly, results require further validations on a larger patient cohort.

Despite this being a preliminary investigation, the possibility of detecting novel loci and germline mutations potentially involved in bAVM onset will allow to hypothesize a strategy for molecular diagnosis, preferably based on a panel of selected genes.

4. Materials and Methods

4.1. Patient Recruitment and WES Analysis

The study was performed on a group of five Italian patients (AVM1–5) diagnosed with bAVM following cerebral angiography investigation (Figure 3). A severity lesion score was assigned to each patient based on the Spetzler–Martin grading system [55]. Anamnestic data are presented in Table 4. No familiar history of bAVM was reported for the patients and they were classified as sporadic. Patients were fully informed on their enrolment in the study and informed consent was obtained, and for underaged patients as well. DNA samples were collected from peripheral blood and purified by the QIAamp DNA Blood Mini Kit (Qiagen). Qualitative and quantitative measurements of the samples were performed by NanoDrop spectrophotometer (Thermo Fisher Scientific) and by a Qubit fluorometer (Thermo Fisher Scientific). Paired-end libraries were obtained by the SureSelect Human All Exon V7 (Agilent) kit and sequenced on a HiSeq 2500 Illumina platform.

Table 4. Anamnesis data of the patients enrolled in the study.

Patient	Sex	Age (Years)	Age of Onset (Years)	Symptoms	Lesion Number	Spetzler–Martin Grading
AVM1	M	14	12	Intracerebral hemorrhage following AVM rupture	1—parietal left area	2
AVM2	M	31	18	Tremor of the left leg, diffuse tremor, seizures	1—front-parietal left area (not bleeding)	2
AVM3	F	32	29	Dizziness, tinnitus, seizures nausea right hemiparesis visus reduction	1—parietal left area	3
AVM4	F	8	At birth	Drowsy status, finalistic limb movement	1—proliferative microangiopathy, central left area	3
AVM5	M	7	5	Sudden headache, vertigo, seizures	1—anterior-parietal paramedian right area	2

The patients are named as mentioned in the text (AVM1–5). Gender, age, and clinical features are reported for each patient. AVM: Arteriovenous malformation. The number (1–5) indicates the sample.

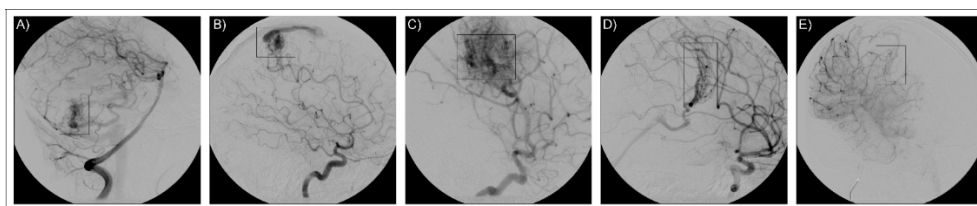


Figure 3. Imaging for neuroradiological diagnosis. The figure reports cerebral angiographies that confirm the presence of bAVM lesions. The five images refer to the five patients as reported in the text: (A) AVM1, (B) AVM2, (C) AVM3, (D) AVM4, (E) AVM5. AVM lesions are framed in the rectangular box.

4.2. Bioinformatic Analysis

FastQ data obtained from sequencing runs were quality checked by the FastQC (v.0.11.7) tool (<http://www.bioinformatics.babraham.ac.uk/projects/fastqc>). Only reads presenting a Phred score ≥ 28 were selected after trimming and aligned to the GRCh38 Human Reference Genome by the Burrows–Wheeler Aligner (BWA) algorithm [56]. Duplicate reads were removed by the MarkDuplicate tool provided by Picard toolkit (v.2.18.23) (“Picard Toolkit.” 2019. Broad Institute, GitHub Repository. <http://broadinstitute.github.io/picard/>; Broad Institute). Then, the Indel realignment and the base recalibration were performed by the Genome Analysis Toolkit (GATK) (v.4.1.3.0) (<https://software.broadinstitute.org/gatk/>). Variant calling was executed by FreeBayes [57], while ANNOVAR v.2018Apr16 [58] was used for variant annotation.

4.3. Variant Filtering Criteria

Before proceeding with downstream analysis, annotated genes and variants were filtered on the basis of several criteria. Variants showing quality score < 150 were discarded. This threshold value was established by the observation that several variants with depth lower than 150 were not confirmed by the following Sanger sequencing validation. Filtered variants were classified by functional class and intronic, synonymous, non-coding RNA, and untranslated regions affecting variants were discarded. Missense, nonsense, frameshift, and short indels presenting an MAF < 0.01 were selected. Rare variants were preferred based on the low worldwide incidence of bAVM. For the MAF-based filtering, the values reported in the Genome Aggregation Database (<https://gnomad.broadinstitute.org/>) [59] and in the 1000 Genomes phase 3 project [60] were considered.

4.4. Gene Clustering and Prioritization

To visualize and functionally group genes carrying filtered variants, the ClueGO plug-in of Cytoscape software was used for each sample [61]. Clustering was performed on the basis of the GO Biological Process, REACTOME and WikiPathways ontologies. Groups showing Bonferroni step down corrected p -value ≤ 0.05 were considered significant and therefore selected for the purpose. Genes within the chosen groups were added to the Test Gene Set in ToppGene (<https://toppgene.cchmc.org/>) [62], a web-based tool for prioritization of candidate genes based on functional similarity to a training gene list. The Training Gene Set group was made up of *ENG*, *ACVRL1*, *TGFBR2*, *SMAD4*, and *GDF2* genes, already known to be causative of HHT and of a few familiar bAVM cases without HHT. The training parameters selected were “GO:Biological Process”, “Human Phenotype”, “Mouse Phenotype”, “Pathway”, “PubMed”, “Interaction”, and “Disease”. Five different analyses were run, one for each exome data. Statistical parameters were calculated applying the Bonferroni correction, and p -values ≤ 0.05 were considered significant.

4.5. Sanger Validation

Variants carried by prioritized genes were validated by Sanger sequencing, next to polymerase chain reaction (PCR) amplification. Primer sequences and PCR conditions are available upon request.

Sanger sequencing was carried out using the BigDyeTerminator[®] v3.1 Cycle Sequencing Kit chemistry and run on a 3130xl Genetic Analyzer (Applied Biosystems, Thermo Fisher Scientific). Moreover, all variants here considered were further searched in an in-house exome-control dataset obtained by WES data, collected on a cohort of 10 Caucasian healthy subjects, heterogeneous for sex and age. The healthy condition was confirmed by computed tomography.

Patients agreed to be enrolled in the study and their informed consents were obtained. The manuscript does not contain information attributable to their identity. The study involves human participants and was approved by the local Ethics Committee “A.O.U. G. Martino”, N.11/2011 date of approval: 14 December.2011.

5. Conclusions

As knowledge on bAVM is still very elusive, we recruited a group of patients affected by sporadic bAVM and performed WES analysis. Clustering of genes which were affected by rare variants highlighted cytoskeleton impairment as well as defective ion conduction in endothelial cells. Therefore, we hypothesize perturbations at these pathways as possible mechanisms involved in bAVM pathogenesis. We prioritized genes more likely linked to lesion development as *FBN2*, *TAB1*, *NCoR2*, *SLIT2*, *RNF111*, *CAMK2B*, *EPHA2*, and *EPHB2*. Although to date no correlation has been reported between gene mutations and clinical phenotype, further characterization of pathways involved in bAVM development could provide a valid criterion to relate molecular features to clinical presentation. In particular, lesion site, bleeding risk, and patient outcome could represent valid prognostic factors linked to patient genotype.

Supplementary Materials: Supplementary materials are available at <http://www.mdpi.com/1422-0067/21/12/4321/s1>. Table S1: AVM Sample Reports of WES Analysis, Table S2: Selected Variants, Table S3: ClueGO Pathways, Table S4: ToppGene Results. Table S5.: STRING Results.

Author Contributions: Conceptualization, C.S.; methodology, C.S., L.D. and C.T.; investigation: M.L. and F.G.; resources: E.M. and A.A.C.; data curation: L.D.; writing—original draft preparation, C.S.; writing—review and editing, A.S.; supervision, R.D. All authors have read and agreed the final version of the manuscript.

Funding: This research received no external funding.

Conflicts of Interest: The authors declare no conflict of interest.

References

1. Winkler, E.A.; Birk, H.; Burkhardt, J.K.; Chen, X.; Yue, J.K.; Guo, D.; Rutledge, W.C.; Lasker, G.F.; Partow, C.; Tihan, T.; et al. Reductions in Brain Pericytes Are Associated With Arteriovenous Malformation Vascular Instability. *J. Neurosurg.* **2018**, *129*, 1464–1474. [[CrossRef](#)] [[PubMed](#)]
2. Ozpinar, A.; Mendez, G.; Abula, A.A. Epidemiology, genetics, pathophysiology, and prognostic classifications of cerebral arteriovenous malformations. *Handb. Clin. Neurol.* **2017**, *143*, 5–13. [[PubMed](#)]
3. Zhang, D.; Zhou, F.; Zhao, X.; Bao, B.; Chen, J.; Yang, J. Endoglin is a conserved regulator of vasculogenesis in zebrafish—Implications for hereditary haemorrhagic telangiectasia. *Biosci. Rep.* **2019**, *39*. [[CrossRef](#)] [[PubMed](#)]
4. Crist, A.M.; Lee, A.R.; Patel, N.R.; Westhoff, D.E.; Meadows, S.M. Vascular Deficiency of Smad4 Causes Arteriovenous Malformations: A Mouse Model of Hereditary Hemorrhagic Telangiectasia. *Angiogenesis* **2018**, *21*, 363–380. [[CrossRef](#)]
5. Wooderchak-Donahue, W.L.; McDonald, J.; O’Fallon, B.; Upton, P.D.; Li, W.; Roman, B.L.; Young, S.; Plant, P.; Fülöp, G.T.; Langa, C.; et al. BMP9 Mutations Cause a Vascular-Anomaly Syndrome With Phenotypic Overlap With Hereditary Hemorrhagic Telangiectasia. *Am. J. Hum. Genet.* **2013**, *93*, 530–537. [[CrossRef](#)]
6. Sasahara, A.; Kasuya, H.; Akagawa, H.; Ujiiie, H.; Kubo, O.; Sasaki, T.; Onda, H.; Sakamoto, Y.; Kriscsek, B.; Hori, T.; et al. Increased expression of ephrin A1 in brain arteriovenous malformation: DNA microarray analysis. *Neurosurg. Rev.* **2007**, *30*, 299–305. [[CrossRef](#)]
7. Bai, J.; Wang, Y.J.; Liu, L.; Zhao, Y.L. Ephrin B2 and EphB4 selectively mark arterial and venous vessels in cerebral arteriovenous malformation. *J. Int. Med. Res.* **2014**, *42*, 405–415. [[CrossRef](#)]

8. Fang, J.; Hirschi, K. Molecular regulation of arteriovenous endothelial cell specification. *F1000Research* **2019**, *8*, F1000 Faculty Rev-1208. [[CrossRef](#)]
9. Vaser, R.; Adusumalli, S.; Leng, S.N.; Sikic, M.; Ng, P.C. SIFT missense predictions for genomes. *Nat. Protoc.* **2016**, *11*, 1–9. [[CrossRef](#)]
10. Schwarz, J.M.; Cooper, D.N.; Schuelke, M.; Seelow, D. MutationTaster2: Mutation prediction for the deep-sequencing age. *Nat. Methods* **2014**, *11*, 361–362. [[CrossRef](#)]
11. Chen, X.; Liu, Y.; Zhou, S.; Nie, S.; Lin, Z.; Zhou, C.; Sun, J.; Gao, X.; Huang, Y. Methylation of the CDKN2A Gene Increases the Risk of Brain Arteriovenous Malformations. *J. Mol. Neurosci.* **2019**, *69*, 316–323. [[CrossRef](#)] [[PubMed](#)]
12. Thomas, J.M.; Surendran, S.; Abraham, M.; Rajavelu, A.; Kartha, C.C. Genetic and epigenetic mechanisms in the development of arteriovenous malformations in the brain. *Clin. Epigenetics* **2016**, *8*, 78. [[CrossRef](#)] [[PubMed](#)]
13. Tual-Chalot, S.; Garcia-Collado, M.; Redgrave, R.E.; Singh, E.; Davison, B.; Park, C.; Lin, H.; Luli, S.; Jin, Y.; Wang, Y.; et al. Loss of Endothelial Endoglin Promotes High-Output Heart Failure Through Peripheral Arteriovenous Shunting Driven by VEGF Signaling. *Circ. Res.* **2020**, *126*, 243–257. [[CrossRef](#)] [[PubMed](#)]
14. Delev, D.; Pavlova, A.; Grote, A.; Boström, A.; Höllig, A.; Schramm, J.; Fimmers, R.; Oldenburg, J.; Simon, M. NOTCH4 gene polymorphisms as potential risk factors for brain arteriovenous malformation development and hemorrhagic presentation. *J. Neurosurg.* **2017**, *126*, 1552–1559. [[CrossRef](#)]
15. Goss, J.A.; Huang, A.Y.; Smith, E.; Konczyk, D.J.; Smits, P.J.; Sudduth, C.L.; Stapleton, C.; Patel, A.; Alexandrescu, S.; Warman, M.L.; et al. Somatic mutations in intracranial arteriovenous malformations. *PLoS ONE* **2019**, *14*, e0226852. [[CrossRef](#)]
16. Al-Olabi, L.; Polubothu, S.; Dowsett, K.; Andrews, K.A.; Stadnik, P.; Joseph, A.P.; Knox, R.; Pittman, A.; Clark, G.; Baird, W.; et al. Mosaic RAS/MAPK Variants Cause Sporadic Vascular Malformations Which Respond to Targeted Therapy. *J. Clin. Investig.* **2018**, *128*, 1496–1508. [[CrossRef](#)]
17. Priemer, D.S.; Vortmeyer, A.O.; Zhang, S.; Chang, H.Y.; Curless, K.L.; Cheng, L. Activating KRAS mutations in arteriovenous malformations of the brain: Frequency and clinicopathologic correlation. *Hum. Pathol.* **2019**, *89*, 33–39. [[CrossRef](#)]
18. Davis, M.R.; Andersson, R.; Severin, J.; de Hoon, M.; Bertin, N.; Baillie, J.K.; Kawaji, H.; Sandelin, A.; Forrest, A.R.; Summers, K.M. FANTOM Consortium: Transcriptional profiling of the human fibrillin/LTBP gene family, key regulators of mesenchymal cell functions. *Mol. Genet. Metab.* **2014**, *112*, 73–83. [[CrossRef](#)]
19. Doetschman, T.; Barnett, J.V.; Runyan, R.B.; Camenisch, T.D.; Heimark, R.L.; Granzier, H.L.; Conway, S.J.; Azhar, M. Transforming growth factor beta signaling in adult cardiovascular diseases and repair. *Cell Tissue Res.* **2012**, *347*, 203–223. [[CrossRef](#)]
20. Vézina, A.; Charfi, C.; Zgheib, A.; Annabi, B. Cerebrovascular Angiogenic Reprogramming upon LRP1 Repression: Impact on Sphingosine-1-Phosphate-Mediated Signaling in Brain Endothelial Cell Chemotactism. *Mol. Neurobiol.* **2018**, *55*, 3551–3563. [[CrossRef](#)]
21. Nakajima, C.; Haffner, P.; Goerke, S.M.; Zurhove, K.; Adelman, G.; Frotscher, M.; Herz, J.; Bock, H.H.; May, P. The lipoprotein receptor LRP1 modulates sphingosine-1-phosphate signaling and is essential for vascular development. *Development* **2014**, *141*, 4513–4525. [[CrossRef](#)] [[PubMed](#)]
22. Grimsey, N.J.; Lin, Y.; Narala, R.; Rada, C.C.; Mejia-Pena, H.; Trejo, J. G protein-coupled receptors activate p38 MAPK via a non-canonical TAB1-TAB2- and TAB1-TAB3-dependent pathway in endothelial cells. *J. Biol. Chem.* **2019**, *294*, 5867–5878. [[CrossRef](#)] [[PubMed](#)]
23. Sylvain-Prévost, S.; Ear, T.; Simard, F.A.; Fortin, C.F.; Dubois, C.M.; Flamand, N.; McDonald, P.P. Activation of TAK1 by Chemotactic and Growth Factors, and Its Impact on Human Neutrophil Signaling and Functional Responses. *J. Immunol.* **2015**, *195*, 5393–5403. [[CrossRef](#)] [[PubMed](#)]
24. Di, Y.; Li, S.; Wang, L.; Zhang, Y.; Dorf, M.E. Homeostatic interactions between MEKK3 and TAK1 involved in NF-kappaB signaling. *Cell. Signal.* **2008**, *20*, 705–713. [[CrossRef](#)]
25. Noshiro, S.; Mikami, T.; Kataoka-Sasaki, Y.; Sasaki, M.; Hashi, K.; Ohtaki, S.; Wanibuchi, M.; Mikuni, N.; Kocsis, J.D.; Honmou, O. Biological relevance of tissue factor and IL-6 in arteriovenous malformations. *Neurosurg. Rev.* **2017**, *40*, 359–367. [[CrossRef](#)]

26. Shoemaker, L.D.; Fuentes, L.F.; Santiago, S.M.; Allen, B.M.; Cook, D.J.; Steinberg, G.K.; Chang, S.D. Human brain arteriovenous malformations express lymphatic-associated genes. *Ann. Clin. Transl. Neurol.* **2014**, *1*, 982–995. [[CrossRef](#)]
27. Murphy, P.A.; Kim, T.N.; Huang, L.; Nielsen, C.M.; Lawton, M.T.; Adams, R.H.; Schaffer, C.B.; Wang, R.A. Constitutively active Notch4 receptor elicits brain arteriovenous malformations through enlargement of capillary-like vessels. *Proc. Natl. Acad. Sci. USA* **2014**, *111*, 18007–18012. [[CrossRef](#)]
28. Hou, Y.; Shin, Y.J.; Han, E.J.; Choi, J.S.; Park, J.M.; Cha, J.H.; Choi, J.Y.; Lee, M.Y. Distribution of vascular endothelial growth factor receptor-3/Flt4 mRNA in adult rat central nervous system. *J. Chem. Neuroanat.* **2011**, *42*, 56–64. [[CrossRef](#)]
29. Chaqour, B. Caught between a “Rho” and a hard place: Are CCN1/CYR61 and CCN2/CTGF the arbiters of microvascular stiffness? *J. Cell Commun. Signal.* **2019**. [[CrossRef](#)]
30. Adams, R.H.; Wilkinson, G.A.; Weiss, C.; Diella, F.; Gale, N.W.; Deutsch, U.; Risau, W.; Klein, R. Roles of ephrinB ligands and EphB receptors in cardiovascular development: Demarcation of arterial/venous domains, vascular morphogenesis, and sprouting angiogenesis. *Genes Dev.* **1999**, *13*, 295–306. [[CrossRef](#)]
31. Liu, H.; Devraj, K.; Möller, K.; Liebner, S.; Hecker, M.; Korff, T. EphrinB-mediated reverse signalling controls junctional integrity and pro-inflammatory differentiation of endothelial cells. *Thromb. Haemost.* **2014**, *112*, 151–163. [[CrossRef](#)] [[PubMed](#)]
32. Zhou, N.; Zhao, W.D.; Liu, D.X.; Liang, Y.; Fang, W.G.; Li, B.; Chen, Y.H. Inactivation of EphA2 promotes tight junction formation and impairs angiogenesis in brain endothelial cells. *Microvasc. Res.* **2011**, *82*, 113–121. [[CrossRef](#)] [[PubMed](#)]
33. Doronzo, G.; Astanina, E.; Corà, D.; Chiabotto, G.; Comunanza, V.; Noghero, A.; Neri, F.; Puliafito, A.; Primo, L.; Spampinato, C.; et al. TFEB controls vascular development by regulating the proliferation of endothelial cells. *EMBO J.* **2019**, *38*, e98250. [[CrossRef](#)] [[PubMed](#)]
34. Kim, J.; Oh, W.J.; Gaiano, N.; Yoshida, Y.; Gu, C. Semaphorin 3E-Plexin-D1 signaling regulates VEGF function in developmental angiogenesis via a feedback mechanism. *Genes Dev.* **2011**, *25*, 1399–1411. [[CrossRef](#)] [[PubMed](#)]
35. Gu, C.; Yoshida, Y.; Livet, J.; Reimert, D.V.; Mann, F.; Merte, J.; Henderson, C.E.; Jessell, T.M.; Kolodkin, A.L.; Ginty, D.D. Semaphorin 3E and plexin-D1 control vascular pattern independently of neuropilins. *Science* **2005**, *307*, 265–268. [[CrossRef](#)]
36. Li, G.J.; Yang, Y.; Yang, G.K.; Wan, J.; Cui, D.L.; Ma, Z.H.; Du, L.J.; Zhang, G.M. Slit2 suppresses endothelial cell proliferation and migration by inhibiting the VEGF-Notch signaling pathway. *Mol. Med. Rep.* **2017**, *15*, 1981–1988. [[CrossRef](#)]
37. Zhang, S.; Kim, J.Y.; Xu, S.; Liu, H.; Yin, M.; Koroleva, M.; Guo, J.; Pei, X.; Jin, Z.G. Endothelial-specific YY1 governs sprouting angiogenesis through directly interacting with RBPJ. *Proc. Natl. Acad. Sci. USA* **2020**, *117*, 4792–4801. [[CrossRef](#)]
38. Koinuma, D.; Shinozaki, M.; Komuro, A.; Goto, K.; Saitoh, M.; Hanyu, A.; Ebina, M.; Nukiwa, T.; Miyazawa, K.; Imamura, T.; et al. Arkadia amplifies TGF-beta superfamily signalling through degradation of Smad7. *EMBO J.* **2003**, *22*, 6458–6470. [[CrossRef](#)]
39. Zhou, P.; Wan, X.; Zou, Y.; Chen, Z.; Zhong, A. Transforming growth factor beta (TGF- β) is activated by the CtBP2-p300-AP1 transcriptional complex in chronic renal failure. *Int. J. Biol. Sci.* **2020**, *16*, 204–215. [[CrossRef](#)]
40. Villa, C.; Colombo, G.; Meneghini, S.; Gotti, C.; Moretti, M.; Ferini-Strambi, L.; Chisci, E.; Giovannoni, R.; Becchetti, A.; Combi, R. CHRNA2 and Nocturnal Frontal Lobe Epilepsy: Identification and Characterization of a Novel Loss of Function Mutation. *Front. Mol. Neurosci.* **2019**, *12*, 17. [[CrossRef](#)]
41. Heeschen, C.; Weis, M.; Aicher, A.; Dimmeler, S.; Cooke, J.P. A novel angiogenic pathway mediated by non-neuronal nicotinic acetylcholine receptors. *J. Clin. Invest.* **2002**, *110*, 527–536. [[CrossRef](#)]
42. Peghaire, C.; Bats, M.L.; Sewduth, R.; Jeanningros, S.; Jaspard, B.; Couffignal, T.; Dupl a, C.; Dufourcq, P. Fzd7 (Frizzled-7) Expressed by Endothelial Cells Controls Blood Vessel Formation Through Wnt/ β -Catenin Canonical Signaling. *Arterioscler. Thromb. Vasc. Biol.* **2016**, *36*, 2369–2380. [[CrossRef](#)]
43. Liu, W.; Rui, H.; Wang, J.; Lin, S.; He, Y.; Chen, M.; Li, Q.; Ye, Z.; Zhang, S.; Chan, S.C.; et al. Axin is a scaffold protein in TGF-beta signaling that promotes degradation of Smad7 by Arkadia. *EMBO J.* **2006**, *25*, 1646–1658. [[CrossRef](#)] [[PubMed](#)]

44. Jensen, L.D.; Hot, B.; Ramsköld, D.; Germano, R.F.V.; Yokota, C.; Giatrellis, S.; Lauschke, V.M.; Hubmacher, D.; Li, M.X.; Hupe, M.; et al. Disruption of the Extracellular Matrix Progressively Impairs Central Nervous System Vascular Maturation Downstream of β -Catenin Signaling. *Arterioscler. Thromb. Vasc. Biol.* **2019**, *39*, 1432–1447. [[CrossRef](#)] [[PubMed](#)]
45. Eisa-Beygi, S.; Benslimane, F.M.; El-Rass, S.; Prabhudesai, S.; Abdelrasoul, M.K.A.; Simpson, P.M.; Yalcin, H.C.; Burrows, P.E.; Ramchandran, R. Characterization of Endothelial Cilia Distribution During Cerebral-Vascular Development in Zebrafish (*Danio rerio*). *Arterioscler. Thromb. Vasc. Biol.* **2018**, *38*, 2806–2818. [[CrossRef](#)] [[PubMed](#)]
46. Noren, D.P.; Chou, W.H.; Lee, S.H.; Qutub, A.A.; Warmflash, A.; Wagner, D.S.; Popel, A.S.; Levchenko, A. Endothelial cells decode VEGF-mediated Ca²⁺ signaling patterns to produce distinct functional responses. *Sci. Signal.* **2016**, *9*, ra20. [[CrossRef](#)] [[PubMed](#)]
47. Yamamura, H.; Suzuki, Y.; Yamamura, H.; Asai, K.; Imaizumi, Y. Hypoxic stress up-regulates Kir2.1 expression and facilitates cell proliferation in brain capillary endothelial cells. *Biochem. Biophys. Res. Commun.* **2016**, *476*, 386–392. [[CrossRef](#)] [[PubMed](#)]
48. Yamazaki, D.; Kito, H.; Yamamoto, S.; Ohya, S.; Yamamura, H.; Asai, K.; Imaizumi, Y. Contribution of K(ir)2 potassium channels to ATP-induced cell death in brain capillary endothelial cells and reconstructed HEK293 cell model. *Am. J. Physiol. Cell. Physiol.* **2011**, *300*, C75–C86. [[CrossRef](#)]
49. Hauer, A.J.; Kleinloog, R.; Giuliani, F.; Rinkel, G.J.E.; de Kort, G.A.; Berkelbach van der Sprenkel, J.W.; van der Zwan, A.; Gosselaar, P.H.; van Rijen, P.C.; de Boer-Bergsma, J.J.; et al. RNA-Sequencing Highlights Inflammation and Impaired Integrity of the Vascular Wall in Brain Arteriovenous Malformations. *Stroke* **2020**, *51*, 268–274. [[CrossRef](#)]
50. Szklarczyk, D.; Gable, A.L.; Lyon, D.; Junge, A.; Wyder, S.; Huerta-Cepas, J.; Simonovic, M.; Doncheva, N.T.; Morris, J.H.; Bork, P.; et al. STRING v11: Protein-protein association networks with increased coverage, supporting functional discovery in genome-wide experimental datasets. *Nucleic Acids Res.* **2019**, *47*, D607–D613. [[CrossRef](#)]
51. Wang, K.; Zhao, S.; Liu, B.; Zhang, Q.; Li, Y.; Liu, J.; Shen, Y.; Ding, X.; Lin, J.; Wu, Y.; et al. Perturbations of BMP/TGF- β and VEGF/VEGFR signalling pathways in non-syndromic sporadic brain arteriovenous malformations (BAVM). *J. Med. Genet.* **2018**, *55*, 675–684. [[CrossRef](#)] [[PubMed](#)]
52. Scimone, C.; Donato, L.; Alafaci, C.; Granata, F.; Rinaldi, C.; Longo, M.; D’Angelo, R.; Sidoti, A. High-Throughput Sequencing to Detect Novel Likely Gene-Disrupting Variants in Pathogenesis of Sporadic Brain Arteriovenous Malformations. *Front. Genet.* **2020**, *11*, 146. [[CrossRef](#)] [[PubMed](#)]
53. Guijarro-Muñoz, I.; Cuesta, A.M.; Alvarez-Cienfuegos, A.; Geng, J.G.; Alvarez-Vallina, L.; Sanz, L. The axonal repellent Slit2 inhibits pericyte migration: Potential implications in angiogenesis. *Exp. Cell Res.* **2012**, *318*, 371–378. [[CrossRef](#)]
54. Harde, E.; Nicholson, L.; Furones Cuadrado, B.; Bissen, D.; Wigge, S.; Urban, S.; Segarra, M.; Ruiz de Almodóvar, C.; Acker-Palmer, A. EphrinB2 regulates VEGFR2 during dendritogenesis and hippocampal circuitry development. *Elife* **2019**, *8*, e49819. [[CrossRef](#)]
55. Spetzler, R.F.; Martin, N.A. A Proposed Grading System for Arteriovenous Malformations. *J. Neurosurg.* **1986**, *65*, 476–483. [[CrossRef](#)] [[PubMed](#)]
56. Li, H.; Durbin, R. Fast and accurate short read alignment with Burrows-Wheeler transform. *Bioinformatics* **2009**, *25*, 1754–1760. [[CrossRef](#)]
57. Garrison, E.; Marth, G. Haplotype-based variant detection from short-read sequencing. *arXiv* **2012**, arXiv:1207.3907v2.
58. Wang, K.; Li, M.; Hakonarson, H. ANNOVAR: Functional annotation of genetic variants from high-throughput sequencing data. *Nucleic Acids Res.* **2010**, *38*, e164. [[CrossRef](#)]
59. Karczewski, K.J.; Francioli, L.C.; Tiao, G.; Cummings, B.B.; Alfoldi, J.; Wang, Q.; Collins, R.L.; Laricchia, K.M.; Ganna, A.; Birnbaum, D.P.; et al. Variation across 141,456 human exomes and genomes reveals the spectrum of loss-of-function intolerance across human protein-coding genes. *BioRxiv* **2019**, 531210. [[CrossRef](#)]
60. 1000 Genomes Project Consortium; Auton, A.; Brooks, L.D.; Durbin, R.M.; Garrison, E.P.; Kang, H.M.; Korbel, J.O.; Marchini, J.L.; McCarthy, S.; McVean, G.A.; et al. A global reference for human genetic variation. *Nature* **2015**, *526*, 68–74.

61. Bindea, G.; Mlecnik, B.; Hackl, H.; Charoentong, P.; Tosolini, M.; Kirilovsky, A.; Fridman, W.H.; Pagès, F.; Trajanoski, Z.; Galon, J. ClueGO: A cytoscape plug-in to decipher functionally grouped gene ontology and pathway annotation networks. *Bioinformatics* **2009**, *25*, 1091–1093. [[CrossRef](#)] [[PubMed](#)]
62. Chen, J.; Bardes, E.E.; Aronow, B.J.; Jegga, A.G. ToppGene Suite for gene list enrichment analysis and candidate gene prioritization. *Nucleic Acids Res.* **2009**, *37*, W305–W311. [[CrossRef](#)] [[PubMed](#)]



© 2020 by the authors. Licensee MDPI, Basel, Switzerland. This article is an open access article distributed under the terms and conditions of the Creative Commons Attribution (CC BY) license (<http://creativecommons.org/licenses/by/4.0/>).